

Human-Vehicle Cooperative Visual Perception for Shared Autonomous Driving

Yiyue Zhao¹, Cailin Lei¹, Yu Shen¹, Yuchuan Du¹, Qijun Chen¹

¹Tongji University

{sc_smile, 2010762, yshen, ycdu, qjchen}@tongji.edu.cn

Abstract

With the development of key technologies like environment perception, the automation level of autonomous vehicles has been increasing. However, before reaching highly autonomous driving, manual driving still need participate in the driving process to ensure the safety of human-vehicle shared driving. The existing human-vehicle cooperative driving focuses on auto engineering and drivers' behaviors, with few research studies in the field of visual perception. Due to the bad performance in the complex road traffic conflict scenarios, cooperative visual perception needs to be studied further. In addition, the autonomous driving perception system cannot correctly understand the characteristics of manual driving. Based on the background above, this paper directly proposes a human-vehicle cooperative visual perception method to enhance the visual perception ability of shared autonomous driving based on the transfer learning method and the image fusion algorithm for the complex road traffic scenarios. Based on transfer learning, the mAP of object detection reaches 75.52% and lays a solid foundation for visual fusion. And the fusion experiment further reveals that human-vehicle cooperative visual perception reflects the riskiest zone and predicts the conflict object's trajectory more precisely. This study pioneers a cooperative visual perception solution for shared autonomous driving and experiments in the real-world complex traffic conflict scenarios, which can better support the following planning and controlling and improve the safety of autonomous vehicles.

1 Introduction

With the development of autonomous driving techniques, automation in the process of driving has increased dramatically. According to research conducted by the Society of Automotive Engineers[1], the automated driving systems could be divided into six levels, from Level-0(fully manual driving) to Level-5(fully automated driving). However, the existing level of automation still maintains at the partially autonomous driving level. Before reaching fully autonomous driving, manual and autonomous driving are required to work together to ensure the safety of driving. Therefore, the safety of human-vehicle cooperative driving has become an important challenge of partially autonomous driving.

Current human-vehicle cooperative driving focuses on be-

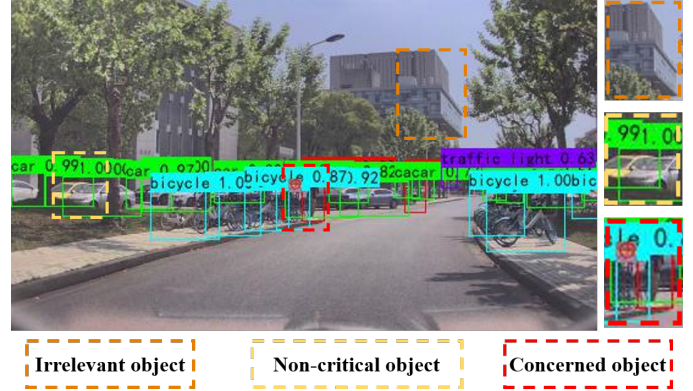


Figure 1: Example of human-vehicle cooperative visual perception. Concerned object is covered by drivers' red gaze point.

haviors of drivers, including applying torque to the steering wheel to stop drivers from turning, giving stimulation when detecting drivers tired, etc.[1][2]. However, existing research seldom studies human-vehicle cooperative driving in the visual perception field. Existing autonomous visual perception algorithms almost predict objects with the same weight so that the system cannot capture the riskiest zone. Thus, there is a large barrier between autonomous visual perception system and drivers' visual features.

To solve the research gaps above, this paper proposes a method in the human-vehicle cooperative visual perception field to enhance the safety of shared autonomous driving based on the transfer learning method and the image fusion algorithm(as shown in Figure 1). The precision of object detection and image fusion are both verified in the real-world road environment. And this study proves that human-vehicle cooperative visual perception performs better than simple autonomous visual perception algorithms in complex traffic scenarios like left-turning traffic collision scenarios, lane change scenarios, and urgent avoidance scenarios[3][4][5].

The main contribution of this paper are as follows:

- (1)We propose a method for in the human-vehicle cooperative visual perception for autonomous vehicles.
- (2)Through visual perception fusion, we can predict the trajectory closer to the actual trajectory, which offers preciser

data support for AVs' planning and controlling.

The rest of this paper is arranged as follows. Section II describe related work about human-vehicle cooperative driving briefly. Section III introduces the method of human-vehicle cooperative visual perception for autonomous driving. Detailed process of experiments is illustrated in Section IV; Section V concludes the results and contributions of the study.

2 RELATED WORK

Human-vehicle cooperative driving has had a certain research foundation since 2005[6]. Despite existing research seldom studies human-vehicle cooperative visual perception, several works have still been explored in hard samples mining.

2.1 Existing Human-vehicle Cooperative Driving Research

Existing studies pay more attention to automatic engineering and drivers' behaviors. In the field of automatic engineering, there are several traditional solutions to assist manual driving from the vehicle perspective. For example, Gazit set an autonomous-mode steering wheel and send a signal to drivers to switch to manual model[7]. In addition, Li proposed a switched cooperative driving model in a cyber-physical perspective to minimize the impact of the transitions between automated and manual driving on traffic operations[8].

On the other hand, drivers' behaviors play an important role in traffic safety. An increasing number of researchers utilize visual, auditory, tactile, and other models to stimulate drivers in the automated mode[9][10][11]. Spence studied tactile and multisensory spatial warning signals on distracted drivers performs better than a simple sensory[12].

In this paper, we use the attentional mechanism as the basis. We refine the advantages of studies on drivers' behaviors and pay attention to human-vehicle cooperative visual perception.

2.2 Existing Visual Perception for Autonomous Driving

Existing autonomous driving visual perception studies includes road traffic scenarios' semantic segmentation and object detection. The former one perceives the road traffic scenario from the global perspective and doesn't care details of every objects' movement situation while the latter one cares more about change of objects' position and movement within a continuous time series. So object detection provides more detailed data for the following planning and controlling[13].

Since 2012, deep learning has become the most powerful techniques to extract objects' features from massive amount of raw data[14][15]. One-stage Detectors like YOLO, SSD have the advantages of fast detection and generalized features extraction while two-stage Detectors such as RCNN, FPN have higher accuracy through region proposal[16][17][18][19]. However, these object detection algorithms cannot adapt to the complex traffic conflict scenarios directly and still need to be optimized.

In this paper, we use object-detection algorithm YoLov4 as the basis and apply transfer learning method to improve the precision and efficiency of detection in the complex road

traffic scenarios, which lays a solid foundation for the further human-vehicle cooperative visual perception.

2.3 Human-vehicle Cooperative Visual Perception for Shared Autonomous Driving

Except for the automatic engineering and drivers' behaviors, visual perception is worth concentrating on in the process of human-vehicle interaction. Traditional autonomous visual perception systems apply cameras to capture road environment images and classify each object with deep learning algorithms. In the whole scenario perception, semantic segmentation is applied widely[20]. Meanwhile, object detection algorithms like YOLO could be utilized to detect dynamic traffic scenarios[21]. On this basis, Kang designed a human-vehicle cooperative navigation system and first simulated visual perception in *SCANeRTM Studio*[22].

In this paper, we absorb the ideas of collecting gaze points of drivers and design experiments in real-world complex traffic scenarios. An image fusion algorithm between gaze points and the camera recorded footage is proposed.

2.4 Image Fusion Techniques

To achieve the drivers' gaze point fused with in-vehicle cameras screen, image fusion techniques play an important role. Traditional image fusion methods include crop and paste operations in Pillow Packages, which can be also achieved in Matplotlib, Scikit-image Packages, etc. However, these methods can easily lose the features of original images and add signal noise into images during the transformation.

In 1987, Gaussian Pyramid was utilized to fuse images, which applied downsample twice to get the minimize resolution images[23]. Through editing frequency band, Gaussian Pyramid can conduct a large-scale research, pre-calculate and image proposal. Similarly, Laplacian Pyramid upsample and smooth the minimize image's layer, and deviate the Gaussian Pyramid in the next layer[24]. By applying Image Pyramid, the detailed pixel information and features can be extracted and maintained, which ensures that images are not distorted during the fusion process.

In this paper, we utilize Gaussian Filter to remove original signal noise first. Then through downsample of Gaussian Pyramid and upsample of Laplacian Pyramid, gaze points are fused with in-vehicle camera screen without missing the original size and features.

3 METHODOLOGYS

In order to improve the perception ability and driving safety for autonomous vehicles in the urgent conflict traffic scenarios, this study proposes a method about human-vehicle cooperative perception.

Cooperative perception includes two steps. First, autonomous driving visual perception system applies object-detection algorithms to detect positions and movement state of objects in the complex road traffic scenarios driving. Due to the uncertainty of transportation participants, current object-detection algorithms cannot adapt to the complex road traffic conflict scenarios. Therefore, this study applies transfer learning method to enhance the detection precision in the complex road traffic conflict scenarios.

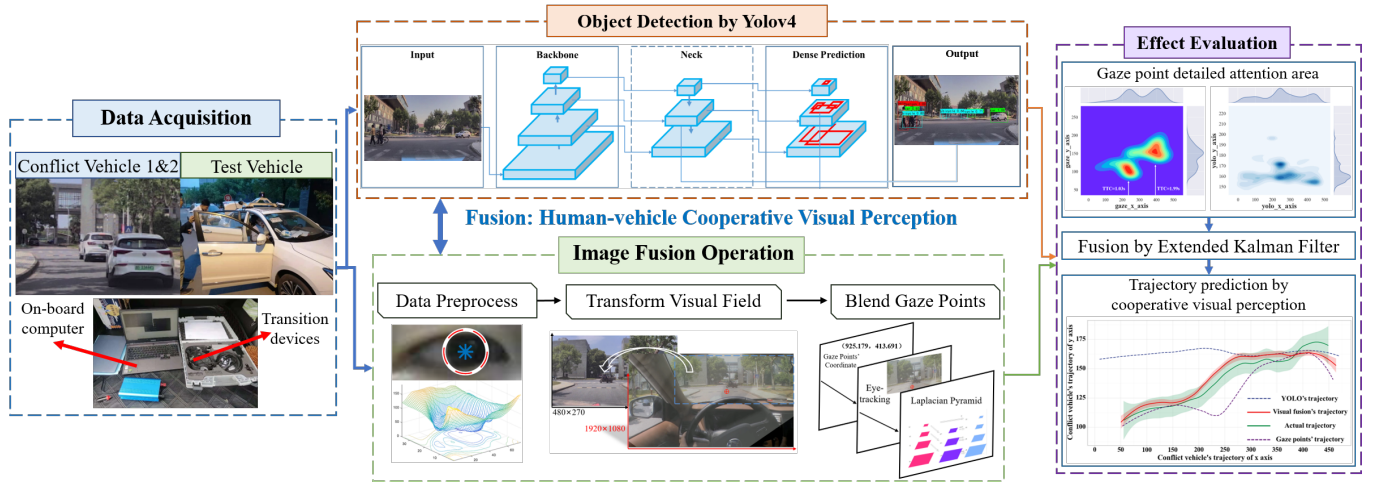


Figure 2: Framework of Human-vehicle Cooperative Perception.

Second, apply image fusion algorithm to merge drivers' gaze points with in-vehicle camera screens which are predicted by object-detection algorithm. Through analyzing the gathering zone of drivers' gaze points, we can obtain the riskiest zone in conflict traffic scenarios, which supports the following planning algorithms to avoid risk better. The framework of this study is shown in Figure 2.

3.1 Data Acquisition on Complex Road Scenarios

To obtain the characteristics of manual driving in real-world complex traffic scenarios and vehicle's real-time movement state, this study acquires three kinds of data:

- Drivers' eye-tracking data
- Scenario tracking data
- Real-time kinematic data

Drivers' eye-tracking data records the location information of drivers' pupil, which can be extracted to obtain the gaze points' characteristics. And the scenario tracking data derives from the screen of in-vehicle cameras, which records the scenarios in front of the experimental vehicle. And the real-time kinematic data records the high-accuracy information of position and movement in the surrounding, including vehicles' relative displacement, speed, acceleration, etc.

3.2 Data Preprocessing

After collecting data in the driving process, this study preprocesses the data further. The scenario tracking data and real-time kinematic data will be transformed in the following data fusion algorithms. In the part, this paper first preprocess the drivers' eye tracking data. By the Canny operator shown as (1), all of the boundary point of pupils can be founded easily.

$$\begin{aligned} \hat{I} &= \sum_{\omega} a_{guid} I_{guid} + b_{guid} \\ a_{guid} &= \frac{\Phi_{\omega}^2}{\Phi_{\omega}^2 + \varepsilon} \\ b_{guid} &= (1 - a_{guid}) M_{\omega} \end{aligned} \quad (1)$$

where

I_{guid} = bootstrap image of the bootstrap filter

\hat{I} = images I_{guid} after filtering

a_{guid}, b_{guid} = linearity coefficient

ω = filter window

M_{ω} = the means of I_{guid} in filter window ω

Φ_{ω} = the variance of I_{guid} in filter window ω

ε = regular term to adjust values of a_{guid}

After detecting the boundary of pupils, we need to determine the location of the pupil center. According to equations of circle: $(x - a)^2 + (y - b)^2 = r^2$, Hough transform finds the circle(a,b,r) that covers most of the boundary point(x,y) in the binary image, then the pupil center coordinate is (a,b) [25]. The Hough transform algorithm is shown below.

Algorithm 1: Pupil Center Coordinate Determination by Hough Transform

Require: L, W, R, x, y, r

- 1: Determine the sizes of input images: L =image.length, W =image.width, $R=\frac{1}{2} \cdot \min(L, W)$.
- 2: Establish three-dimensional array (L, W, R) and calculate the number of boundary points (x, y) of each parameter circle.
- 3: Iterate all boundary points of images, compute circle equations of each boundary point, and record the results into the array: $(x, y) \rightarrow (L, W, R) \rightarrow (L, W, R)$.
- 4: Count circle parameters' number, and find the maximum one (i.e., the Hough circle): $(x - a)^2 + (y - b)^2 = r^2$.
- 5: Return the pupil center coordinate (L, W, R) .

Through **Algorithm 1**, the pupil center's location of two eyes is determined. Averaging two pupils' center coordinate, we obtain the preprocessing gaze point, which is convenient for the following cooperative visual perception.

3.3 Data Fusion Algorithms

To achieve the human-vehicle cooperative visual perception, this paper establish data fusion algorithms between in-vehicle screens after object-detection and drivers' gaze points.

Object Detection of Complex Road Traffic Scenario

Before achieving human-vehicle cooperative visual perception, we need detect complex road traffic scenarios based on transfer learning [26]. Transfer learning migrates pre-trained parameters from the source domain to the target domain, which can effectively utilize the learning results of the pre-trained model. Thus, the training process requires a smaller volume of datasets and can rapidly improve the efficiency.

Through looking up references, the accuracy of object detection would decline dramatically with scenarios' complexity increasing[27]. Therefore, we apply the transfer learning method to make algorithms better adapt to complex scenarios after verify object-detection algorithms' accessibility. Detailed methods could be divided into two steps:

Step 1: migrate initial data to the complex traffic scenario dataset. Because the pre-trained model is trained based on the Coco dataset (an object dataset including 80 classes), it cannot adapt to our complex road traffic scenario dataset perfectly. Thus, we're supposed to establish the connection of categories between the two datasets, including the "many-to-one" mapping relationship and the "one-to-one" derivation relationship, as shown in Figure 3.

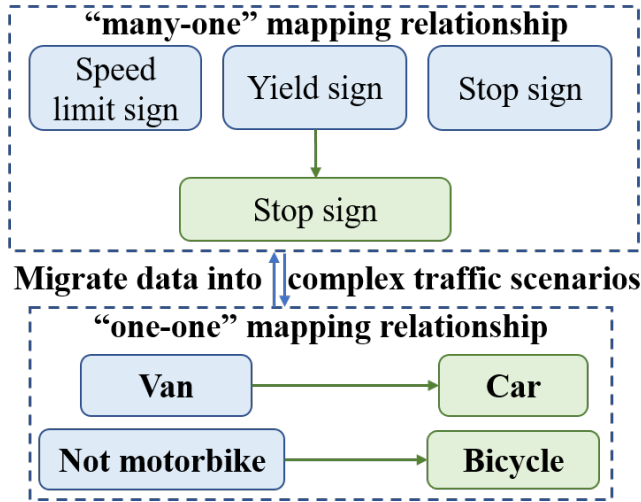


Figure 3: Data Migration between Coco dataset and complex traffic scenario dataset.

Step 2: optimize the hyper-parameters of the pre-trained model. Due to the large size of objects in the Coco dataset, the pre-trained model hardly recognizes small-size objects in a complex road traffic scenario. Therefore, we optimize the hyper-parameters in the pre-trained model to improve training efficiency and accuracy, as shown in TABLE 1[28][29].

Image fusion Algorithms

Through data preprocessing, we can get the center coordinate (x_i, y_i) of the human gaze point. By measuring the pixel

Table 1: Optimal Hyper-parameters and Improving Effect

Optimal Hyper-parameter	Improving Effect
Input size:608×608	Improve boundary accuracy
Regular term: $\alpha = 10^{-4}$	Prevent overfitting
Learning rate:Cosine anneal	Find the optimal solution fast
Mosaic augmentation	Recognize small-size object
label smoothing:0.005	Reduce classifying wrong
Add CIOU to improve loss	Stabilize the target box

size of the gaze point, the gaze point is a circle that the circle center coordinate is (x_i, y_i) and radius is 35 pixels. With the Crop function in Pillow (the third package of Python), human gaze points in eye-tracking videos can be distracted frame by frame. And crop box will be transformed in coordinate telescoping as shown in (2).

$$\begin{aligned}
 x_j &= \frac{(x_i - 480)x_1}{x_0 - x_1} \pm \frac{35x_1}{2x_0} (\text{min takes -,max takes +}) \\
 y_j &= \frac{(y_i - 10)y_1}{y_0 - y_1} \pm \frac{35y_1}{2y_0} (\text{min takes -,max takes +})
 \end{aligned} \quad (2)$$

where

x_0 =horizontal axis pixel value of eye-tracking screen
 x_1 =horizontal axis pixel value of in-vehicle screen
 y_0 =vertical axis pixel value of eye-tracking screen
 y_1 =vertical axis pixel value of in-vehicle screen
 x_i =horizontal coordinate of the gaze point
 y_i =vertical coordinate of the gaze point

Then we capture the area of eye tracking images arranging from $[x_{jmin} : x_{jmax}, y_{jmin} : y_{jmax}]$ and apply Laplacian of Gaussian (LoG) to smooth the signals n_r, n_c (the length and width of images) from eye-tracking images. The detailed Gaussian Filter[23] is shown as (3).

$$\begin{aligned}
 LoG(x, y) &= \nabla^2 G_\sigma(x, y) \\
 &= \frac{\partial^2 G_\sigma(x, y)}{\partial x^2} + \frac{\partial^2 G_\sigma(x, y)}{\partial y^2} \\
 &= -\frac{1}{\pi\sigma^4} e^{-\frac{x^2+y^2}{2\sigma^2}} \left(1 - \frac{x^2+y^2}{2\sigma^2}\right) \quad (3)
 \end{aligned}$$

Then executing Algorithm 2 below, we can construct Gaussian and Laplacian Pyramid[24] and fuse drivers' gaze points of eye-tracking image B with in-vehicle camera screen A after object detection.

3.4 Data Postprocessing and Prediction

The precise object detection of traffic scenarios and fused images can be further applied to analyze manual eye-tracking characteristics in the process of driving. The object covered by the drivers' gaze point will be given a larger weight, which makes the visual perception system better perceive the riskiest zone in complex traffic scenarios such as left-turning traffic collision scenarios, lane change scenarios, emergency

Algorithm 2: Image fusion Algorithm-Image Pyramid

Require: n_c, n_r, A, B

- 1: Downscale B twice when iterating over the image of the previous layer until the DPI reaches minimization to construct Gaussian Pyramid of B : $n'_r = \frac{n_r}{2^n}, n'_c = \frac{n_c}{2^n}$.
 - 2: Upscale and smooth the minimized images, deteriorate images of the upper level in Gaussian Pyramid until the image's size is equal to the initial image: $LB = B.laplacian_pyramid$
 - 3: Repeat the above operation to obtain the Laplace pyramid of A : $LA = A.laplacian_pyramid$
 - 4: Operate binary mask for B to get interested area (i.e., gaze point): $M = B.mask$
 - 5: Repeat step 1. to get Gaussian Pyramid of M : $GM = M.gaussian_pyramid$
 - 6: Use GM nodes as weights and synthesiz Laplace Pyramid LS from LA and LB : $LS(i, j) = GM(i, j) \cdot LA(i, j) + (1 - GM(i, j)) \cdot LB(i, j)$
 - 7: Reconstruct pyramid LS to return fused images S :
 $S = \text{reconstruct_image_from_laplacian_pyramid}(LS)$
-

avoidance scenarios of pedestrians, etc. Through Expand Kalman Filter algorithm, human-vehicle cooperative visual perception can fuse the characteristics of manual eye-tracking data and object detection algorithms, which can predict the trajectory of conflict vehicles better and provide more accurate data for the following planning and controlling session of autonomous vehicles.

4 EXPERIMENT

4.1 Setup

The experiment invites nineteen volunteers of different driving experiences to drive the semi-autonomous vehicle produced by HONDA. This paper acquired data in Tongji University during 8th and 9th May 2021, covering sunny and cloudy conditions. Participants were required to wear eye tracking device Dikablis Professional Glasses 3.0, as shown in Figure 4. We could track pupils' movement during experiment, especially in complex traffic scenarios like left-turning traffic conflict scenarios, lane change scenarios, and urgent avoidance scenarios of pedestrians. And this device could record pupils' position data and send back at every 0.117s.

In addition, variables of sensors are installed on the experimental vehicle. In-vehicle camera from Robosense records the scenario in front of the experimental vehicle. Real-time kinematic (RTK) from Robosense can send back the vehicles' state information in real-time including vehicles' relative displacement, absolute speed and acceleration, free space away from the sidewalk, the distance of deviation from lane center line in the scenarios.

To achieve cooperative visual perception and acquire manual eye-tracking features in variables of traffic scenarios, this experiment sets up six driving scenarios, including three

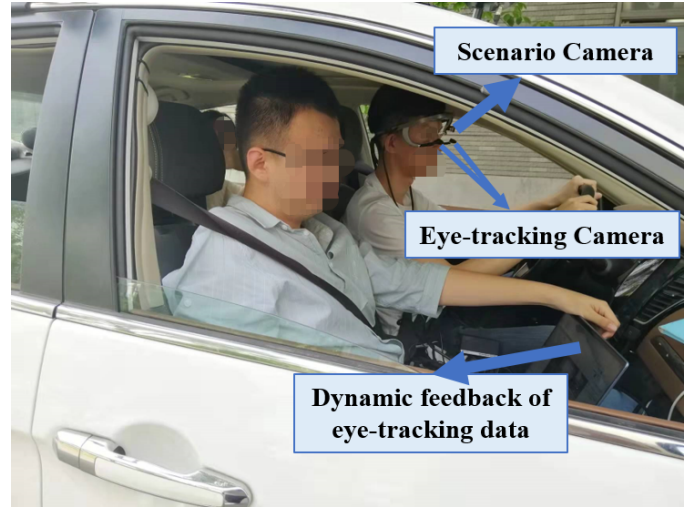


Figure 4: Eye-tracking Device: Dikablis Professional Glasses.

conflict scenarios(left-turning traffic conflict scenarios, lane change scenarios, and urgent avoidance scenarios of pedestrians.), as shown in Table 2.

Table 2: Experimental Scenario Design

Experiment number	Driving Scenarios
1	Straight driving
2	Turn left or right without obstacles
3	Vehicle-vehicle conflict at the cross
4	Two-vehicle or three-vehicle following
5	Conflict between pedestrian and vehicle
6	Conflict between non-motorized vehicles and motorized vehicles

The detailed experimental scenario is located in Tongji University, Shanghai. According to the driving scenarios in Table 2, the experiment selects a closed route in the campus. And the detailed experimental designs including driving route and conflict scenarios, are illustrated in Figure 5.

Then this study invites 18 volunteers to participate the experiment, including 9 male and 10 female(M=21 years, Std=1.1 years). The participants' driving experience arranges from 0.5 to 5 year(M=1.875 years, Std=0.75 years).

18 participants are divided into three groups, and there are not obvious demographic differences of participants among these three groups. The first group just need to tackle the vehicle-vehicle conflict in No.3 experiment, and the second group need to deal with conflict between pedestrian and vehicle in No.5 experiment, while the third group need to solve the conflict between not-motorized vehicles and motorized vehicles in No.6 experiment .

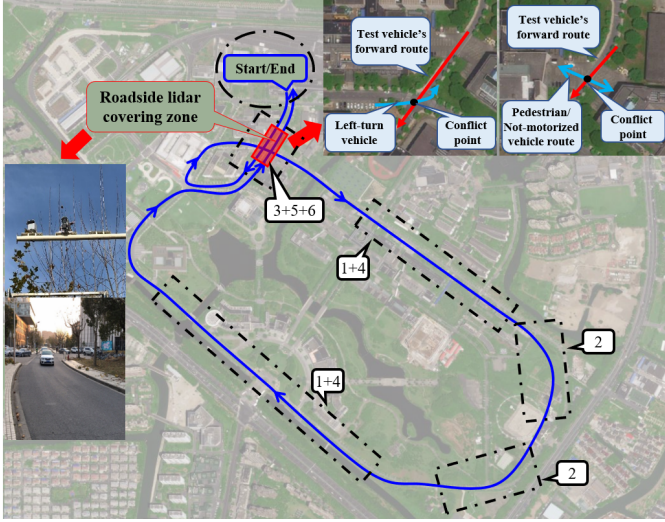


Figure 5: Illustration of the detailed experimental scenario.

4.2 Object Detection of Vehicle's Visual Perception

Dataset

Due to the advantages of transfer learning, the required scale of the dataset is small. This paper distracted 505 images cover complex traffic scenarios like left-turning traffic collision scenarios, lane change scenarios, and emergency avoidance scenarios of pedestrians. Then we draw rectangles to label objects' class shown in Figure 3 manually.

Training Detail

When training, divides the dataset into train-set and validation-set by 9:1 randomly. The improved backbone of the model is CSPDarkNet53 while activate function is justified to Mish, as shown in (4).

$$Mish = x \cdot \tanh(\ln(1 + e^x)) \quad (4)$$

And the feature enhancement extraction network adds Spatial Pyramid Pooling (SPP) and PANet, which are capable to greatly increase the perceptual field, repeatedly extract features, and isolate the most significant contextual features. In addition, the pre-trained weight comes from the training weight of the Coco dataset.

Evaluation Metrics

The metrics for evaluation include the mean of each of these values: F1-score, Precision Rate, Recall Rate, and Average Precision (AP). mAP, the mean value of AP, has become a common metric to evaluate results of multi-classification tasks. It can be calculated by (5).

$$AP = \frac{1}{11} \sum_{r \in \{0, 0.1, \dots, 1\}} P_{interp}(r) \quad (5)$$

$$mAP = \frac{\sum_{q=1}^Q AP(q)}{Q}$$

Loss Study

To validate the accessibility of the pre-trained model, we apply the pre-trained weight of the Coco dataset to train the Coco dataset. And the loss result in the process of iterating is shown in Figure 6.

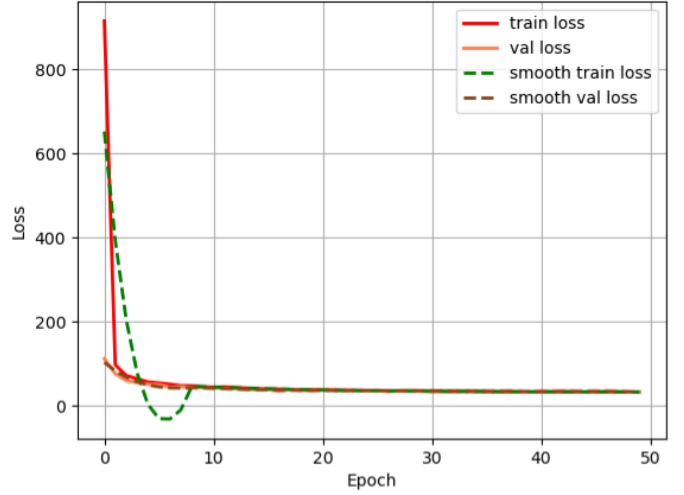


Figure 6: Loss of pre-trained model with Coco_weight.

As shown in Figure 6, the pre-trained model converges fast and the mAP of the Coco dataset is 69.3%, which ranks in the upper level in the existing open-source algorithms. Thus, the pre-trained model is accessible to detect more complex traffic scenarios.

Detection Algorithm Improvement by Transfer Learning

This part will improve the framework of the pre-trained model by transfer learning, to make it better adapt to complex traffic scenarios.

After validating the accessibility of the pre-trained model, we apply it to predict our dataset directly. The mAP of twelve classes remains 41.7%, and the problems of missing or wrong prediction are exposed. To improve the accuracy and efficiency of the pre-trained model, we set control experiments including six experimental groups and one control group. Through adjusting hyperparameters of the pre-trained model in order(as shown in TABLE 1), we record the predicted mAP of each group. The contrast result is shown in Figure 7.

As shown in Figure7, it's obvious to find the effect of transfer learning. The mAP is improved from 41.7% of the pre-trained model to 75.8%. And in the complex road traffic scenarios, mosaic data augmentation and input size expansion improve the predicted precision most effectively. Then the current object-detection algorithms can distinguish different objects in the complex road traffic scenarios, which lays a solid foundation for human-vehicle cooperative visual perception in the urgent conflict scenarios.

4.3 Manual Gaze Point Fusion

To better percept the conflict object in the urgent traffic scenarios for autonomous vehicles, visual perception system

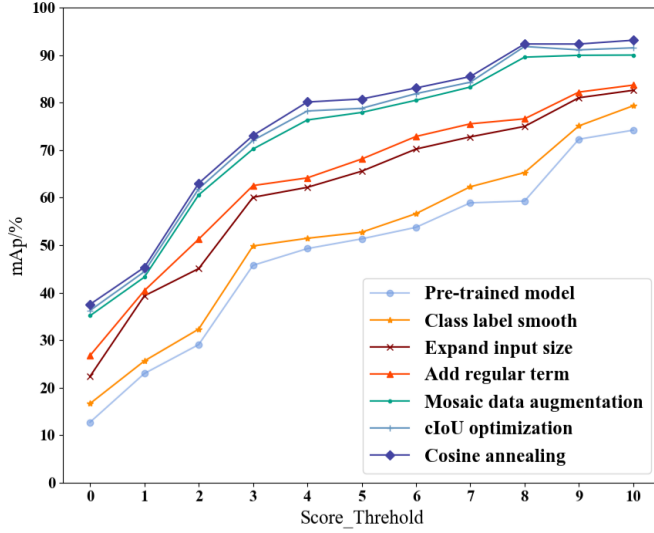


Figure 7: Framework improvement by transfer learning.

should learn which zone is the riskiest (meanwhile the gathering zone of drivers' gaze points), instead of regarding interaction object as a particle. So this study fuses drivers' gaze points with in-vehicle camera screen after object detection, to detect the riskiest zone in the interaction process. The detailed process can be divided into three steps:

Gaze Point Data Preprocessing

In the process of the experiment, eye-tracking device records pupils' changes dynamically. To gain the location of gaze points, we need preprocess pupils' data first.

Compared with Laplacian Operator and Laplacian of Gaussian Operator(LoG), Canny Operator applies Non-Maximum Suppression Algorithm(NMS) to detect the optimal edge of pupils[30]. Through Canny Operator, we can detect pupils' edge precisely and suppress signals' noise, which remains the characteristics of pupils best, as shown in Figure 8.

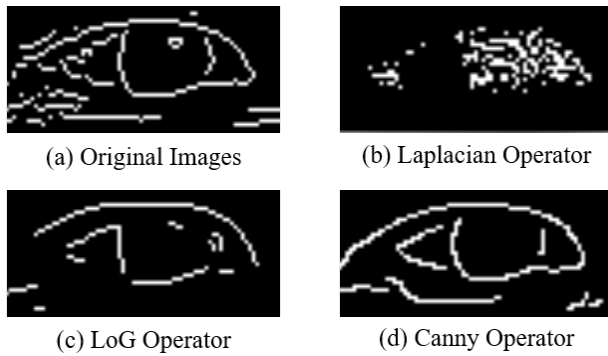


Figure 8: Comparison of output images of pupils by different detection operators.

After detecting the pupils' edge, we need identify pupils' center to obtain precise gaze point further. In this study, we regard pupil as a circle. Through Hough Transform and all of

the edge points detected by Canny Operator, the center point and area of pupils could be obtained easily. Part of data samples are shown in TABLE 3.

Table 3: Data samples of pupils' center coordinate and area

UTC	Gaze_X	Gaze_Y	Pupils' Area
1620436346002	945.955	350.986	267.106
1620436346018	944.948	345.331	266.902
1620436346035	949.124	346.003	267.213
1620436346052	950.346	353.577	267.342
1620436346068	952.838	343.551	267.554
1620436346085	954.279	348.433	267.753
1620436346102	953.835	339.682	267.687
1620436346118	952.794	343.375	267.587
1620436346135	951.404	332.533	267.474
1620436346152	950.233	334.493	267.293

Through Canny Operator and Hough Transform, system feeds the coordinate information of gaze points to receive side dynamically, which provide data support for the following gaze points fusion.

Coordinate Conversion of Visual Field

Considering visual field of in-vehicle camera screen different from eye-tracking screen, and there is wobble on the eye-tracking device. When drivers' gaze points fused with in-vehicle camera screen, we need coverse coordinate according to in-vehicle camera screen.

Through coordinate transform Equation2, we can converse coordinate of the eye-tracking screen (whose size is 1920×1080) to the coordinate of in-vehicle camera (whose size is 480×270). Then drivers' visual field is identical to the in-vehicle camera screen.

Gaze Point Extraction and fusion

Through reading coordinate information of pupils, we can collect the center of gaze points and set 70×70 pixels squares to crop gaze points from eye-tracking screen. Then we add Gaussian Filter to remove signal noise and remain characteristics of gaze points by Laplace Pyramid. Finally, we apply Equation 2 to fuse the smoothed gaze points with in-vehicle camera screen.

Through three steps above, we can fuse gaze points with in-vehicle camera screen successfully. And the example of gaze point fusion with in-vehicle camera screen in a left-turn conflict scenario is shown in Figure 9

4.4 Ground-truth processing

To verify the advantages of human-vehicle cooperative visual perception for autonomous driving, this paper introduces Real-time Kinetic(RTK) data to compare. Because the results of human-vehicle visual perception are 2D images, this paper transformed relative displacement in real-world road into pixel-level trajectory to validate in the same coordinate. The

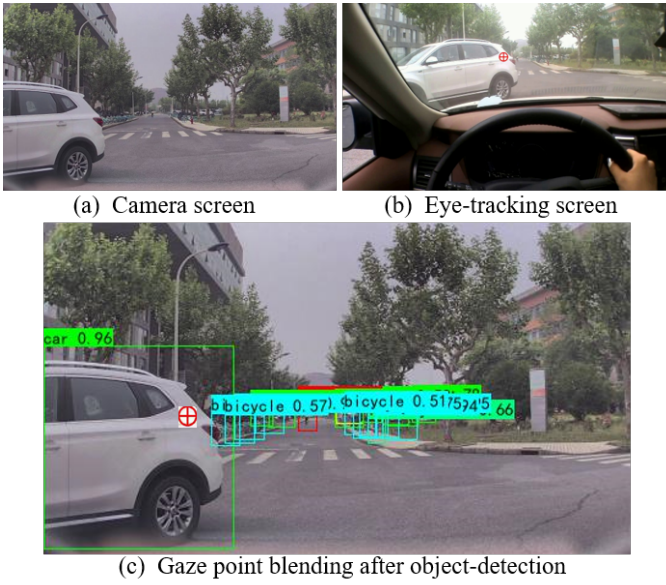


Figure 9: Example of image fusion.

transforming formula is shown as Equation 6.

$$\begin{aligned} p_{x_j} &= \frac{s_{x_2} - s_{x_1}}{p_{x_2} - p_{x_1}} \cdot \frac{(x_i - 480)x_1}{x_0 - x_1} \cdot s_{x_j} \\ p_{y_j} &= \frac{s_{y_2} - s_{y_1}}{p_{y_2} - p_{y_1}} \cdot \frac{(y_i - 10)y_1}{y_0 - y_1} \cdot s_{y_j} \end{aligned} \quad (6)$$

where

p_{x_j} =horizontal axis pixel value of actual trajectory of conflict vehicle

p_{y_j} =vertical axis pixel value of actual trajectory of conflict vehicle

s_{x_j} =horizontal axis value of actual trajectory of conflict vehicle in real world

s_{y_j} =vertical axis value of actual trajectory of conflict vehicle in real world

4.5 Effect Validation of Human-vehicle Cooperative Visual Perception

After fusion gaze points with in-vehicle camera screen, we need validate the effect of human-vehicle cooperative visual perception and explore differences of visual characteristics between machines' perception system and manual drivers.

Experimental Scenario

This study selects the left-turn conflict scenario to validate the effect of human-vehicle cooperative visual perception through gaze point fusion. The experimental scenario is set up as shown in Figure 10. The test vehicle moves forward while another vehicle turns left suddenly at the cross.

And the RTK returns the state of the experimental vehicle and the closest conflict object dynamically.

As shown in Figure 11, we can gain the detailed speed and acceleration change of test vehicles. Additionally, RTK devices also provide the speed of the closest conflict objects

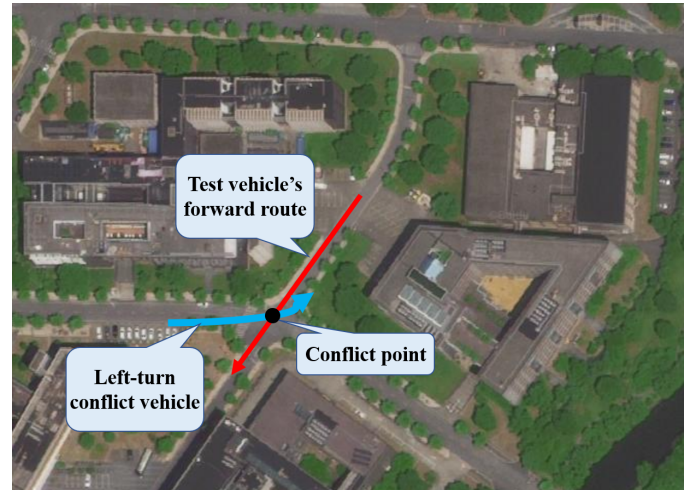


Figure 10: Human-vehicle cooperative perception validation in the left-turn conflict scenario.

and the distance between test vehicles and the closest conflict objects.

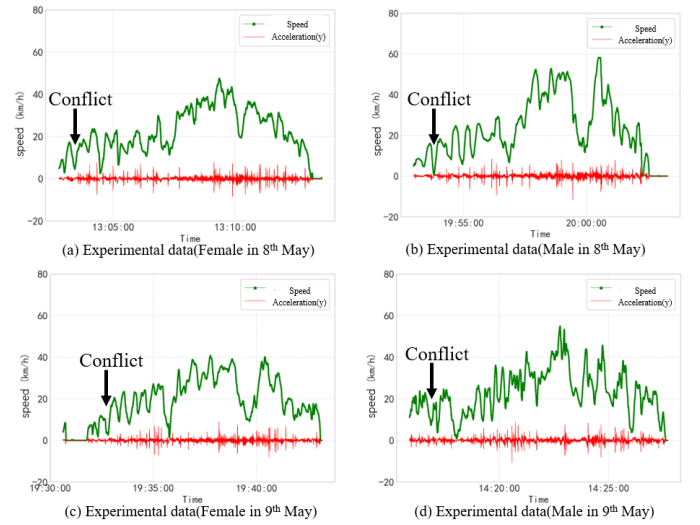


Figure 11: Changes of speed and acceleration in y direction in four experiments.

Evaluation Metrics

TTC (Time to Collision) measures the urgent degree in the conflict scenario. First order of TTC can be calculated by Equation 7:

$$TTC = \frac{\Delta S}{\Delta v} \quad (7)$$

where:

ΔS = Distance between test vehicles and conflict object

Δv = Relative Speed derivation in y direction

In left-turn conflict scenarios, $\Delta v = v_{1y} + v_{2y}$. And v_{1y}, v_{2y} indicate the speed in y direction of test vehicle and

left-turn conflict vehicles. Then we can obtain gathering zone of gaze points in different TTC conditions.

Trajectory and Attentive Zone of Human's Gaze Points

This study collects 36 left-turn conflict scenarios of 18 participants like Figure 10 and sums their eye-tracking data up. And the distribution of drivers' gaze points and anchors' center of Yolo are obtained, the comparison between human's gaze points and vehicle's visual perception is shown in Figure 12.

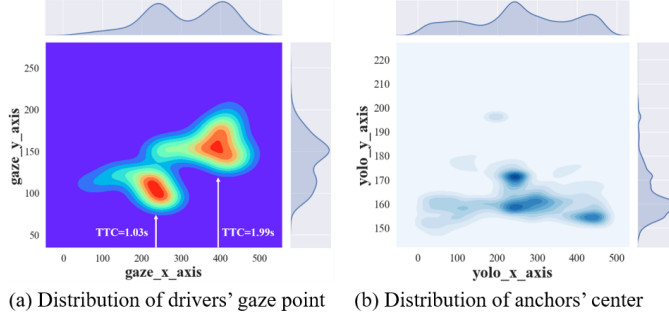


Figure 12: Differences between drivers' gaze zone and object detection zone by Yolo.

From Figure 12, we can find when TTC is beyond 2.0s, drivers' gaze points locate out of the closest conflict vehicles. When TTC declines below 2.0s, drivers tend to care farther zone of the conflict car (like the rear tire of vehicles) while $TTC \leq 1.03s$, drivers tend to care the closet zone away from them, as shown in Figure 12(a). On the contrast, distribution of predicted anchors' center almost remains at a certain height, without obvious attentive zone in left-turn conflict scenarios.

Unlike existing object detection algorithms identifying conflict objects' positions by the center point of predicted anchors, human-vehicle coordinate visual perception cares detailed contour position of conflict objects, which always indicates the riskiest zone in the complex conflict traffic scenarios. To better improve ability of visual perception for autonomous vehicles, it's essential to fuse gaze points and object detection result.

Trajectory prediction

Based on the result above, this paper further verifies the correctness and validation of cooperative visual perception through comparing the actual ground-truth trajectory and the trajectory after visual fusion.

- Actual trajectory

Through transforming real-world relative displacement into pixel-level trajectory by Equation 6, we can compare the trajectory prediction effect with it at the same coordinate axis.

- Gaze points' trajectory
- Yolo's trajectory

Based on the trajectory of gaze points and yolo, this paper applies Extended Kalman Filter(EKF) to fuse these two tra-

jectory as the predicted trajectory of the conflict object. The Extended Kalman Filter design is shown as Equation 8.

$$\begin{aligned}\hat{z}_{k+1} &= h(\hat{x}_{k+1|k}) \\ \hat{x}_{k+1|k+1} &= \hat{x}_{k+1} + K_{k+1}(z_{k+1} - \hat{z}_{k+1|k}) \\ \hat{x}_{k+1} &= f(\hat{x}_{k|k}) \\ K_{k+1} &= P_{k+1|k} H_{k+1}^T (H_{k+1} P_{k+1|k} H_{k+1}^T + R_{k+1})^{-1} \\ P_{k+1|k} &= F_k P_k F_k^T + Q_k \\ P_{k+1|k+1} &= (I - K_{k+1} H_{k+1}) P_{k+1|k}\end{aligned}\quad (8)$$

where

- $x_{k|k}$: state estimate value at the moment k
- z_{k+1} : measured vector value at the moment $k + 1$
- $f(x_k)$: non-linear function of state vector
- $h(x_k)$: non-linear function of measured vector
- $P_{k+1|k}$: state estimate covariance at the moment $k + 1$
- K_{k+1} : state matrix at the moment $k + 1$
- F_k : partial derivative of $f(x_k)$ to x at the moment k
- H_k : partial derivative of $h(x_k)$ to x at the moment k

Based on the non-linear function $f(x_k)$ of state vector x_k (including gaze points' trajectory and yolo's trajectory) and non-linear function $h(x_k)$ of measured vector z_k (fusion trajectory), we can approximate the next state estimate z_{k+1} of the system through Kalman Filter algorithm. And the trajectory prediction result is shown in Figure 13.

We can easily find that the red smooth line of visual fusion's trajectory is closer to the actual trajectory in green than Yolo's trajectory and gaze points' trajectory alone. And the Root Mean Squared Error (RMSE) of predicted trajectory is 0.88 pixel, proving the accuracy of predicted trajectory.

Then we can conclude that cooperative visual perception can better predict the conflict object's trajectory and support the following planning and controlling session for autonomous vehicles.

5 CONCLUSION

In this work, we propose a method in the human-vehicle cooperative visual perception field to enhance visual perception ability of shared autonomous driving.

A complex road traffic scenario detection based on YoLov4 and transfer learning is designed. The detection network migrates data from Coco dataset to the complex traffic scenario and optimizes the hyper-parameters of CSPDarkNet53. And its benefits for the complex road traffic scenario detection results have been proved by experiments.

A fusion technique between drivers' gaze points and in-vehicle camera screen is also designed. Existing object detection algorithms identify objects by the center of predicted anchors, which ignores the drivers' visual characteristics. This study fuses drivers' gaze points and object detection results, and the fusion method is evaluated on the left-turn conflict experiment. It can predict the conflict object's trajectory accurately.

The proposed method shows that human-vehicle cooperative visual perception reflects the riskiest zone in the complex conflict traffic scenarios and predicts more precise trajectory

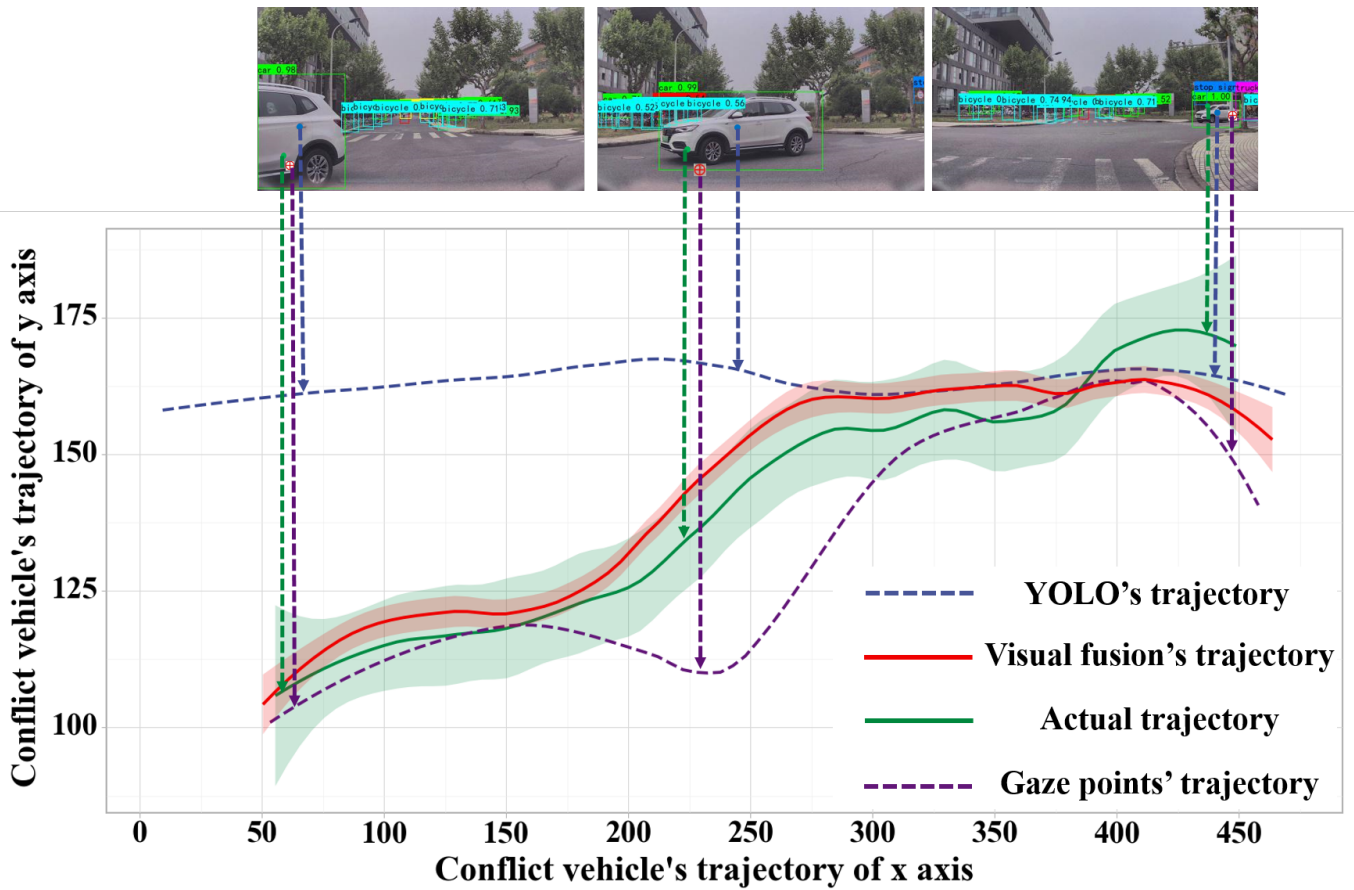


Figure 13: Actual trajectory and predicted trajectory after visual fusion.

of the conflict object, which benefits the following human-vehicle cooperative planning and controlling.

For the future research, we plan to add gyroscope onto the eye-tracking devices to record driver's sitting position and head orientation change. Then we can identify more precise position of drivers' gaze points and promote the accuracy and efficiency of human-vehicle cooperative visual perception.

Acknowledgment

This study is sponsored by the National Key Research and Development Program of China under Grant No. 2020AAA0108100.

References

- [1] F. Biondi, I. Alvarez, and J. Kyeong-Ah, "Human-vehicle cooperation in automated driving: A multidisciplinary review and appraisal," *International Journal of Human-Computer Interaction*, vol. 35, no. 11, pp. 932-46, 2019.
- [2] S. Satardekar, D. Shah, R. Badugu, A. Pawar, and P. Chawan, "Distracted driver detection and classification," *International Journal of Engineering Research and Application*, vol. 8, no. 4, III, pp. 60-64, 04/01 2018.
- [3] E. Dabbour and S. Easa, "Proposed collision warning system for right-turning vehicles at two-way stop-controlled rural intersections," *Transportation Research Part C: Emerging Technologies*, vol. 42, pp. 121-131, 05/01/ 2014.
- [4] N. Kalra and S. M. Paddock, "Driving to safety: How many miles of driving would it take to demonstrate autonomous vehicle reliability?," *Transportation Research Part A Policy & Practice*, vol. 94, no. dec., pp. 182-193, 2016.
- [5] W. Yang, X. Zhang, Q. Lei, and X. Cheng, "Research on longitudinal active collision avoidance of autonomous emergency braking pedestrian system (AEB-P)," *Sensors (Basel, Switzerland)*, vol. 19, no. 21, 2019.
- [6] R. Ma and D. Kaber, "Situation awareness and workload in driving while using adaptive cruise control and a cell phone," *International Journal of Industrial Ergonomics*, vol. 35, no. 10, pp. 939-953, 2005.
- [7] R. Y. Gazit, "Steering wheels for vehicle control in manual and autonomous driving," *U.S. Patent 20130002416 A1*, 2013.
- [8] Y. Li, D. Sun, M. Zhao, D. Chen, S. Cheng, and F. Xie, "Switched cooperative driving model towards human

vehicle copilot situation: A cyberphysical perspective," *Journal of Advanced Transportation*, vol.20,no.18, 2018.

- [9] C. Gold and K. Bengler, "Taking over control from highly automated vehicles," *Human Factors and Ergonomics Society Annual Meeting Proceedings*, vol. 8, no. 64, 2014.
- [10] I. Politis, S. Brewster, and F. Pollick, "Language-Based multimodal displays for the handover of control in autonomous cars," in *Proceedings of the 7th International Conference on Automotive User Interfaces and Interactive Vehicular Applications*, 2015.
- [11] T. Ziemke, K. E. Schaefer, and M. Endsley, "Situation awareness in human-machine interactive systems," *Cognitive Systems Research*, vol. 46, no. dec., pp. 1-2, 2017.
- [12] C. Spence, "Tactile and multisensory spatial warning signals for drivers," *IEEE Trans Haptics*, vol. 1, no. 2, pp. 121-129, 2008.
- [13] C. B. Murthy, M. F. Hashmi, N. D. Bokde, and Z. W. Geem, "Investigations of Object Detection in Images/Videos Using Various Deep Learning Techniques and Embedded Platforms-A Comprehensive Review," *Applied Sciences-Basel*, vol. 10, no. 9, May 2020, Art no. 3280, doi: 10.3390/app10093280.
- [14] LeCun, Y.; Bengio, Y.; Hinton, G. Deep learning. *Nature* 2015, 521, 436–444.
- [15] Hinton, G.E.; Salakhutdinov, R.R. Reducing the dimensionality of data with neural networks. *Science* 2006, 313, 504–507.
- [16] Redmon, J.; Divvala, S.; Girshick, R.; Farhadi, A. You only look once: Unified, real-time object detection. In *Proceedings of the Conference on Computer Vision and Pattern Recognition*, Las Vegas, NV, USA, 26 June–1 July 2016; pp. 779–788.
- [17] Liu, W.; Anguelov, D.; Erhan, D.; Szegedy, C.; Reed, S.; Fu, C.Y.; Berg, A.C. SSD: Single shot multibox detector. In *Proceedings of the European Conference on Computer Vision*, Amsterdam, The Netherlands, 8–16 October 2016; Springer: Berlin, Germany, 2016; pp. 21–37.
- [18] Girshick, R.; Donahue, J.; Darrell, T.; Malik, J. Rich feature hierarchies for accurate object detection and semantic segmentation. In *Proceedings of the Conference on Computer Vision and Pattern Recognition*, Columbus, OH, USA, 24–27 June 2014; pp. 580–587.
- [19] Lin, T.Y.; Dollár, P.; Girshick, R.; He, K.; Hariharan, B.; Belongie, S. Feature pyramid networks for object detection. In *Proceedings of the Conference on Computer Vision and Pattern Recognition*, Honolulu, HI, USA, 21–26 July 2017; pp. 2117–2125.
- [20] J. Shotton, M. Johnson, and R. Cipolla, "Semantic texture forests for image categorization and segmentation," *Proceedings IEEE Computer Vision and Pattern Recognition*, vol. 5, no. 7, pp. 1-8, 2008.
- [21] A. Bochkovskiy, C. Y. Wang, and H. Liao, "YOLOv4: Optimal speed and accuracy of object detection," in *IEEE Computer Vision and Pattern Recognition*, 2020.
- [22] K. Yue and A. C. Victorino, "Human-vehicle cooperative driving using image-based dynamic window approach: System design and simulation," in *2016 IEEE 19th International Conference on Intelligent Transportation Systems (ITSC)*, 2016.
- [23] Z. Tao, D. Mu, and S. Ren, "Information hiding (IH) algorithm based on Gaussian Pyramid and GHM (Geronimo Hardin Massopust) multi-wavelet transformation," *International Journal of Digital Content Technology & Its Applications*, vol. 5, no. 3, pp. 210-218, 2011.
- [24] P. J. Burt and E. H. Adelson, "The Laplacian Pyramid as a compact image code," *Readings in Computer Vision*, vol. 31, no. 4, pp. 671-679, 1987.
- [25] D. H. Ballard, "Generalizing the Hough Transform to detect arbitrary shapes - ScienceDirect," *Readings in Computer Vision*, pp. 714-725, 1987.
- [26] A. Lazaric, "Transfer in reinforcement learning: a framework and a survey." Springer Berlin Heidelberg, 2012.
- [27] SON,T. T., Mita S., Takeuchi A.. "Road Detection using Segmentation by Weighted Aggregation based on Visual Information and a Posteriori Probability of Road Regions". 2008 IEEE International Conference on Systems, Man and Cybernetics. New York.2008,30,17-24.
- [28] I. Loshchilov and F. Hutter, "SGDR: Stochastic gradient descent with warm restarts," in *ICLR 2017 (5th International Conference on Learning Representations)*, 2016.
- [29] T. Ngogia, Y. Li, D. Jin, J. Guo, and Q. Tang, "Real-time sea cucumber detection based on YOLOv4-Tiny and Transfer Learning using data augmentation," in *Advances in Swarm Intelligence, 12th International Conference, ICSI 2021, Proceedings, Part II, Qingdao, China, July 17–21 2021*.
- [30] Y. Zhang, "Research on Driver's State Detection and Application on Man-Machine Shared Driving, " Chongqing University, Chongqing, 2018.